Hindawi
Advances in High Energy Physics
Volume 2019, Article ID 6870793, 13 pages
https://doi.org/10.1155/2019/6870793

Research Article

Anti-de-Sitter-Maxwell-Yang-Mills Black Holes Thermodynamics from Nonlocal Observables Point of View

H. El Moumni [1,2]

[1] *EPTHE, Physics Department, Faculty of Sciences, Ibn Zohr University, Agadir, Morocco*
[2] *High Energy Physics and Astrophysics Laboratory, Faculty of Science Semlalia, Cadi Ayyad University, 40000 Marrakesh, Morocco*

Correspondence should be addressed to H. El Moumni; hasan.elmoumni@edu.uca.ma

Received 29 June 2018; Revised 28 October 2018; Accepted 23 December 2018; Published 20 January 2019

Guest Editor: Saibal Ray

In this paper we analyze the thermodynamic properties of the Anti-de-Sitter black hole in the Einstein-Maxwell-Yang-Mills-AdS gravity (EMYM) via many approaches and in different thermodynamical ensembles (canonical/grand canonical). First, we give a concise overview of this phase structure in the entropy-thermal diagram for fixed charges and then we investigate this thermodynamical structure in fixed potentials ensemble. The next relevant step is recalling the nonlocal observables such as holographic entanglement entropy and two-point correlation function to show that both observables exhibit a Van der Waals-like behavior in our numerical accuracy and just near the critical line as the case of the thermal entropy for fixed charges by checking Maxwell's equal area law and the critical exponent. In the light of the grand canonical ensemble, we also find a newly phase structure for such a black hole where the critical behavior disappears in the thermal picture as well as in the holographic one.

1. Introduction

Over the last years, a great emphasis has been put on the application of the Anti-de-Sitter/conformal field theory correspondence [1, 2] which plays a pivotal role in recent developments of many physical themes [3–5]; in this particular context the thermodynamics of Anti-de-Sitter black holes become more attractive for investigation [6].

In general, black hole thermodynamics has emerged as a fascinating laboratory for testing the predictions of candidate theories of quantum gravity. It has been figured that black holes are associated thermodynamically with a entropy and a temperature [7] and a pressure [8]. This association has led to a rich structure of phase picture and a remarkable critical behavior similar to van der Waals liquid/gas phase transition [9–19]. Another confirmation of this similarity appears when we employ nonlocal observables such as entanglement entropy, Wilson loop, two-point correlation function, and the complexity growth rate [20–33]. Meanwhile, these tools are used extensively in quantum information and to characterize phases and thermodynamical behavior [21, 23, 34–41].

The black hole charge finds a deep interpretation in the context of the AdS/CFT correspondence linked to condensed matter physics; the charged black hole introduces a charge density/chemical potential and temperature in the quantum field theory defined on the boundary [42]. In this background, the charged black hole can be viewed as an uncondensed unstable phase which develops a scalar hair at low temperature and breaks $U(1)$ symmetry near the black hole horizon reminiscing the second-order phase transition between conductor and superconductor phases [43]; this situation is called the "s-wave" holographic superconductor. It has also been shown that "p-wave" holographic superconductor corresponds to vector hair models [44, 45]. The simplest example of p-wave holographic superconductors may be provided by an Einstein-Yang-Mills theory with $SU(2)$ gauge group and no scalar fields, where the electromagnetic gauge symmetry is identified with an $U(1)$ subgroup of $SU(2)$. The other components of the $SU(2)$ gauge field play the role of charged fields dual to some vector operators that break the $U(1)$ symmetry, leading to a phase transition in the dual field theory.

Motived by all the ideas described above, although the Yang-Mills fields are confined to acting inside nuclei while the Maxwell field dominates outside, the consideration of such theory where the two kinds of field live is encouraged by the existence of exotic and highly dense matter in our universe. In this work, we try to contribute to this rich area by revisiting the phase transition of Anti-de-Sitter black holes in Einstein-Maxwell-Yang-Mills (EMYM) gravity. More especially, we investigate the first- and second-order phase transition by different approaches including the holographic one and in different canonical ensembles.

This work is organized as follow: First, we present some thermodynamic properties and phase structure of the EMYM-AdS black holes in (temperature, entropy)-plane in canonical and grand canonical ensemble. Next, we show in Section 3 that the holographic approach exhibits the same behavior; in other words we recall the entanglement entropy and two-point correlation function to check the Maxwell's equal area law and calculate the critical exponent of the specific heat capacity which is consistent with that of the mean field theory of the Van der Waals in the canonical ensemble near the critical point. In the grand canonical one, a new phase structure arises where the critical behavior disappears in the thermal as well as the holographic framework. The last section is devoted to a conclusion.

2. Critical Behavior of Einstein-Maxwell-Yang-Mills-AdS Black Holes in Thermal Picture

2.1. Canonical Ensemble. We start this section by writing the N-dimensional for Einstein-Maxwell-Yang-Mills gravity with a cosmological constant Λ described by the following action [46, 47]

$$\mathcal{I} = \frac{1}{2}\int_{\mathcal{M}} dx^N \sqrt{-g}\left(R - \frac{(N-1)(N-2)}{3}\Lambda - \mathcal{F}_M - \mathcal{F}_{YM}\right), \tag{1}$$

where R is the Ricci scalar while Λ is the cosmological constant. Also $\mathcal{F}_M = F_{\mu\nu}F^{\mu\nu}$ and $\mathcal{F}_{YM} = \mathbf{Tr}(F^{(a)}_{\mu\nu}F^{(a)\mu\nu})$ are the Maxwell invariant and the Yang-Mills invariant, respectively; the trace element stands for $\mathbf{Tr}(.) = \sum_{a=1}^{(N-1)(N-2)/2}(.)$. Varying the action (1) with respect to the metric tensor $g_{\mu\nu}$, the Faraday tensor $F_{\mu\nu}$, and the YM tensor $F^{(a)}_{\mu\nu}$, one can obtain the following field equations

$$G_{\mu\nu} + \Lambda g_{\mu\nu} = T^M_{\mu\nu} + T^{YM}_{\mu\nu} \tag{2}$$

$$\nabla F^{\mu\nu} = 0 \tag{3}$$

$$\widehat{D}_\mu F^{(a)}_{\mu\nu} = \nabla_\mu F^{(a)\mu\nu} + \frac{1}{\Theta}\varepsilon^{(a)}_{(b)(c)}A^{(b)}_\mu F^{(c)\mu\nu} = 0 \tag{4}$$

where $G_{\mu\nu}$ is the Einstein tensor, the quantity $\varepsilon^{(a)}_{(b)(c)}$'s stands for the structure constants of the $((N-1)(N-2)/2)$-parameters Lie group G, Θ is coupling constant, and $A^{(a)}_\mu$ denotes the $SO(N-1)$ gauge groupe YM potential. We also note that the internal indices $\{a, b, c, \cdots\}$ do not differ whether in covariant or contravariant form. In addition, $T^M_{\mu\nu}$ and $T^{YM}_{\mu\nu}$ are the energy momentum tensor of Maxwell and YM fields with the following formula

$$T^M_{\mu\nu} = -\frac{1}{2}g_{\mu\nu}F_{\rho\sigma}F^{\rho\sigma} + 2F_{\mu\lambda}F^\lambda_\nu \tag{5}$$

$$T^{YM}_{\mu\nu} = \sum_{a=1}^{(N-1)(N-2)/2}\left[-\frac{1}{2}g_{\mu\nu}F^{(a)}_{\rho\sigma}F^{(a)\rho\sigma} + 2F^{(a)}_{\mu\lambda}F^{(a)\lambda}_\nu\right] \tag{6}$$

$$F^{(a)}_{\mu\nu} = \partial_\mu A^{(a)}_\nu - \partial_\nu A^{(a)}_\mu + \frac{1}{2\Theta}\varepsilon^{(a)}_{(b)(c)}A^b_\mu A^c_\nu, \tag{7}$$

$$F_{\mu\nu} = \partial_\mu A_\nu - \partial_\nu A_\mu. \tag{8}$$

where A_μ is the usual Maxwell potential. The metric for such N dimensional spherical black hole may be chosen to be [47]

$$ds^2 = -f(r)\,dt^2 + \frac{1}{f(r)}dr^2 + r^2 d\Omega_n^2 \tag{9}$$

in which $d\Omega_n^2$ represents the volume of the unit n-sphere which can be expressed in the standard spherical form

$$d\Omega^2_{N-2} = d\theta_1^2 + \sum_{i=2}^{N-3}\Pi_{j=1}^{i-1}\sin^2\theta_j d\theta_i^2 \quad \text{where } 0 \le \theta_1 \le \pi,\ 0 \le \theta_i \le 2\pi. \tag{10}$$

In order to find the electromagnetic field, we recall the following radial gauge potential ansatz $A_\mu = h(r)\delta^0_\mu$ which obeys the Maxwell field equations (3) with the following solution

$$\frac{dh(r)}{dr} = \frac{c}{r^{N-2}} \tag{11}$$

where c is an integration constant related to electric charge C of the solutions. To solve the YM field, (4), we use the magnetic Wu–Yang ansatz of the gauge potential [48, 49] given by

$$A^{(a)} = \frac{Q}{r^2}\left(x_i dx_j - x_j dx_i\right), \quad 2 \le i \le N-1, \quad 1 \le j \le i-1, \quad 1 \le (a) \le \frac{(N-1)(N-2)}{2} \tag{12}$$

where we imply (to have a systematic process) that the super indices a are chosen according to the values of i and j in order. For instance, we present some of them

$$\begin{aligned}
A^{(1)} &= \frac{Q}{r^2}\left(x_2dx_1 - x_1dx_2\right)\\
A^{(2)} &= \frac{Q}{r^2}\left(x_3dx_1 - x_1dx_3\right)\\
A^{(3)} &= \frac{Q}{r^2}\left(x_3dx_2 - x_2dx_3\right)\\
A^{(4)} &= \frac{Q}{r^2}\left(x_4dx_1 - x_1dx_4\right)\\
A^{(5)} &= \frac{Q}{r^2}\left(x_4dx_2 - x_2dx_4\right)\\
A^{(6)} &= \frac{Q}{r^2}\left(x_4dx_3 - x_3dx_4\right)\\
A^{(7)} &= \frac{Q}{r^2}\left(x_5dx_1 - x_1dx_5\right)\\
A^{(8)} &= \frac{Q}{r^2}\left(x_5dx_2 - x_2dx_5\right)\\
A^{(9)} &= \frac{Q}{r^2}\left(x_5dx_3 - x_3dx_5\right)\\
A^{(10)} &= \frac{Q}{r^2}\left(x_5dx_4 - x_4dx_5\right)\\
&\cdots
\end{aligned} \tag{13}$$

in which $r^2 = \sum_{i=1}^{N-1} x_i^2$. The YM field 2-forms are defined by the expression

$$F^{(a)} = dA^{(a)} + \frac{1}{2Q}\varepsilon^{(a)}_{(b)(c)}A^{(b)} \wedge A^{(c)}. \tag{14}$$

In general for N we must have $(N-1)(N-2)/2$ gauge potentials. The integrability conditions

$$dF^{(a)} + \frac{1}{Q}\varepsilon^{(a)}_{(b)(c)}A^{(b)} \wedge F^{(c)} = 0 \tag{15}$$

are easily satisfied by using (28). The YM equations

$$d * F^{(a)} + \frac{1}{Q}\varepsilon^{(a)}_{(b)(c)}A^{(b)} \wedge *F^{(c)} = 0 \tag{16}$$

also are all satisfied. The energy-momentum tensor (4) becomes after

$$\sum_{a=1}^{(N-1)(N-2)/2}\left[F^{(a)}_{\lambda\sigma}F^{(a)\lambda\sigma}\right] = \frac{(N-3)(N-2)Q^2}{r^4} \tag{17}$$

with the nonzero components

$$\begin{aligned}
T_{00} &= \frac{(N-3)(N-2)Q^2 f(r)}{2r^4}\\
T_{11} &= -\frac{(N-3)(N-2)Q^2}{2r^4 f(r)}\\
T_{22} &= -\frac{(N-3)(N-6)Q^2}{2r^2}\\
T_{AA} &= -\frac{(N-3)(N-6)Q^2}{2r^2}\Pi_{i=1}^{A-2}\sin^2\theta_i\\
&2 < A \le N-1.
\end{aligned} \tag{18}$$

Using (2) and after some simplifications, one can find that the metric function $f(r)$ has the following form given by

$$f(r) = 1 - \frac{2m}{r^{n-1}} - \frac{\Lambda}{3}r^2 + \frac{2(n-1)C^2}{nr^{2n-2}} - \frac{(n-1)Q^2}{(n-3)r^2}, \tag{19}$$

where $N = n + 2$; one can note in the particular case for $n = 3$ that the last term of (19) diverges, involving an unusual logarithmic term in Yang-Mills charge [46]. For this gravity background the parameter m is related to the mass of such black hole, while C and Q are the charges of Maxwell field and Yang-Mills field, respectively. Following previous literature [8, 9], one can find a close connection between the cosmological constant and pressure as $P = -\Lambda/8\pi$, leading to the following expressions of Hawking temperature, mass, and entropy of such black hole in terms of the horizon radius r_+

$$\begin{aligned}
T &= \frac{f'(r_+)}{4\pi} = \frac{n-1}{4\pi r_+} + \frac{2(n+1)P}{3}r_+ - \frac{(n-1)Q^2}{4\pi r^3}\\
&\quad - \frac{(n-1)^2C^2}{2\pi n r_+^{2n-1}},
\end{aligned} \tag{20}$$

$$\begin{aligned}
M &= \frac{n\omega_n}{48\pi}\left(8\pi P r_+^{n+1} + \frac{3(n-1)Q^2r^{n-3}}{3-n} + 3r_+^{n-1}\right.\\
&\quad \left. + \frac{6(n-1)C^2}{nr_+^{n-1}}\right),
\end{aligned} \tag{21}$$

$$S = \frac{\omega_n r_+^n}{4}, \tag{22}$$

The Yang-Mills potential Φ_Q and the electromagnetic one Φ_C can be written as

$$\Phi_Q = \left(\frac{\partial M}{\partial Q}\right)_{C,P,r_+} = \frac{\omega_n(n-1)nQ}{8\pi(3-n)}r_+^{n-3}, \tag{23}$$

$$\Phi_C = \left(\frac{\partial M}{\partial C}\right)_{Q,P,r_+} = \frac{\omega_n(n-1)C}{4\pi r_+^{n-1}}, \tag{24}$$

where $\omega_n = 2\pi^{(n+1)/2}/\Gamma((n+1)/2)$ is the volume of the unit n-sphere. In fact, according to the interpretation of the black

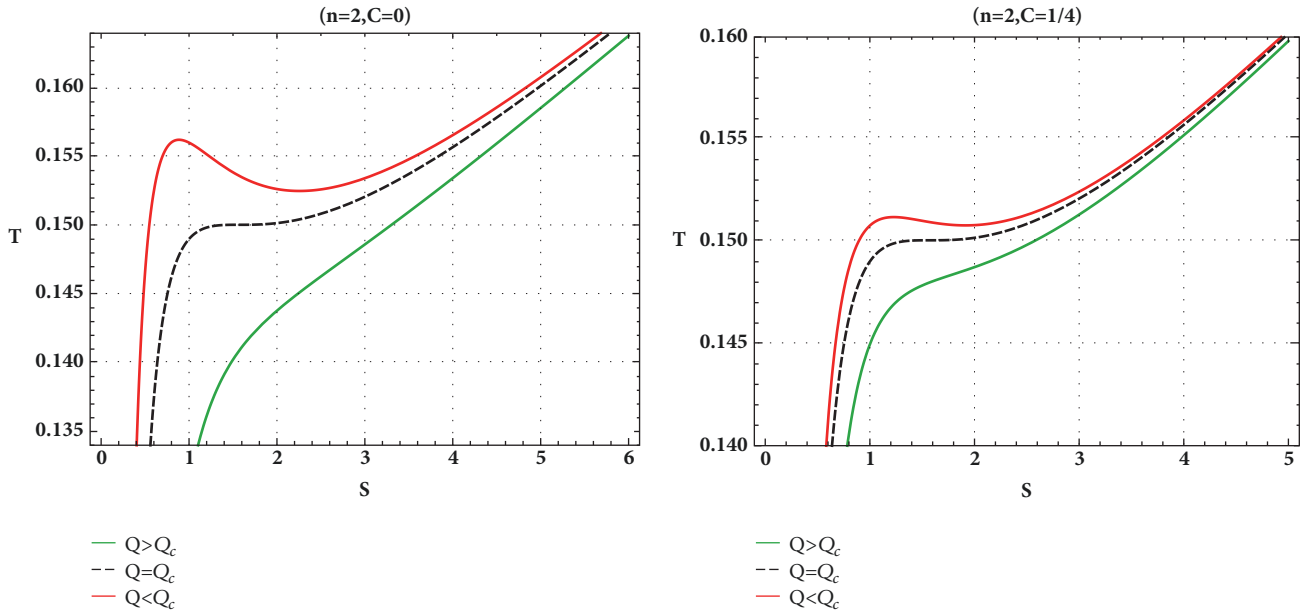

FIGURE 1: The temperature as a function of the entropy for different values of charge C. **(Left)** $C = 0$. **(Right)** $C \neq 0$.

hole mass M as an enthalpy [8] in the extended phase space context, the free energy $\mathcal{F}$ of black hole can be written as

$$\mathcal{F} = M - T \cdot S \tag{25}$$

and the heat capacity is given by

$$C_Q = T \frac{\partial S}{\partial T}\bigg|_Q \tag{26}$$

It is straightforward to show that obtained quantities (20), (21), and (22) obey the first law of black hole thermodynamics in the extended phase space

$$dM = TdS + \Phi_Q dQ + \Phi_C dC + VdP, \tag{27}$$

where V is the Legendre transform of the pressure, which denotes the thermodynamic volume with

$$V = \left(\frac{\partial M}{\partial P}\right)_{S,\Phi_Q,\Phi_C} = \frac{n\omega_n \pi}{3} r^{n+1}. \tag{28}$$

In addition to this, using scaling argument, the corresponding Smarr formula is

$$M = \frac{n}{n-1} TS + \Phi_C C + \frac{1}{(n-1)} \Phi_Q Q - \frac{2}{n-1} VP. \tag{29}$$

Without loss of generality, inserting (22) into (20), we can get the entropy Hawking temperature relation of such black hole, namely,

$$\begin{aligned} T = \frac{1}{12\pi n} \Bigg[& 6C (n-1)^2 \left(4^{1/n} \left(\frac{S}{\omega_n}\right)^{1/n}\right)^{1-2n} \\ & + \pi 2^{2/n+3} n (n+1) P \left(\frac{S}{\omega_n}\right)^{1/n} \\ & - 3 (n-1) n Q^2 4^{-3/n} \left(\frac{S}{\omega_n}\right)^{-3/n} \\ & + 3\, 4^{-1/n} (n-1) n \left(\frac{S}{\omega_n}\right)^{-1/n} \Bigg] \end{aligned} \tag{30}$$

This relation is depicted in Figure 1; indeed it has been shown that there is a Van der Waals-like phase transition; furthermore a direct confirmation comes from the solution of the following system

$$\left(\frac{\partial T}{\partial S}\right)_Q = \left(\frac{\partial^2 T}{\partial S^2}\right)_Q = 0. \tag{31}$$

which reveal the existence of a critical point. The critical charge, entropy, and temperature are given in Table 1; for all the rest of the paper we keep $n = 2$.

An important remark that can be observed here is that both quantities T_c and S_c are insensible with the charge C. The behavior of the free energy $\mathcal{F}$ with respect to the temperature may be investigated by plotting in Figure 2 the graph $\mathcal{F} - T$ for a fixed value of charge Q under the critical one. From

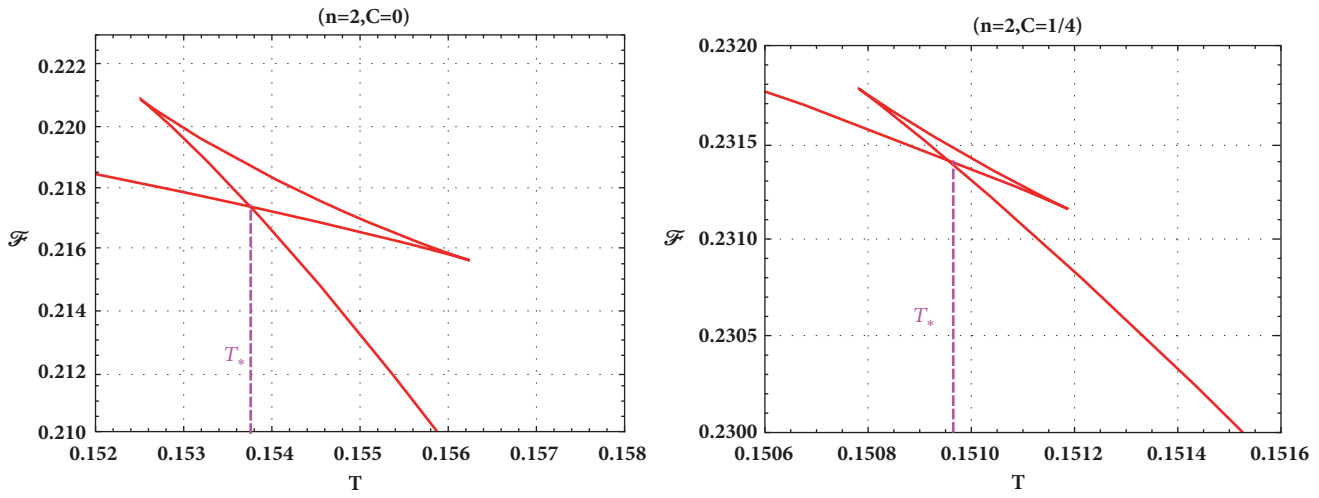

Figure 2: The Helmholtz free energy in function of the entropy for EMYM-AdS black holes for different values of the charge C. **(Left)** $C = 0$. **(Right)** $C \neq 0$.

Table 1: Coordinates of the critical points for different values of C in (T, S)-diagram.

	Q_c	S_c	T_c
C = 0	$\frac{1}{2\sqrt{3}}$	$\frac{\pi}{2}$	$\frac{\sqrt{2}}{3\pi}$
C ≠ 0	$\frac{1}{6}\sqrt{3 - 36C^2}$	$\frac{\pi}{2}$	$\frac{\sqrt{2}}{3\pi}$

Table 2: Check of the equal area law in the $T - S$ plane for different C.

C	$T_\star$	S_1	S_2	S_3	A_1	A_2
0	0.15376	0.638237	1.52994	3.13241	0.383499	0.38350
$\frac{1}{4}$	150965	1.05043	11.54616	2.25932	00.18248	0.1825

this plot, we can observe the characteristic swallow-tail which guarantees the existence of the Van der Waals-like phase transition.

Using Figure 2, we can derive numerically the coexistence temperature $T_\star$ needed in the Maxwell's equal area law construction

$$A_1 \equiv \int_{S_1}^{S_2} T(S)\, dS - T_\star (S_2 - S_1)$$
$$= T_\star (S_3 - S_2) - \int_{S_2}^{S_3} T(S)\, dS \equiv A_2, \tag{32}$$

where S_3, S_2, and S_1 are the solutions of $T(S) = T_\star$ in descending order, in addition to the numerical values of these points, and we report in Table 2 the areas A_1 and A_2 in Maxwell's law (32)

Obviously, the area A_1 equals area A_2 for different C, so the equal area law does not break. For the second phase transition, we know that, near the critical point, there is always a linear relation with slope equal to 3 [47, 50]

$$\log|T - T_c| = 3\log|S - S_c| + constant \tag{33}$$

in this context, the heat capacity behaves like

$$C_Q \sim (T - T_c)^{-2/3} \tag{34}$$

where the critical exponent of the second-order phase is −2/3, which is consistent with the mean field theory.

2.2. Grand Canonical Ensemble. Having described the thermodynamical behavior of the EMYM-AdS black hole with a fixed charge, by showing the occurrence of the first and second phase transition, we will focus this section on the phase structure when the potentials are kept fixed.

To facilitate the calculation of relevant quantities, it is convenient to reexpress the Hawking temperature as a function of entropy, Yang-Mills, and electromagnetic potentials, inserting (23) and (24) into (30); one can write

$$T = \frac{1}{3\pi 2^{2(n+1)/n}} \left(\frac{S}{\omega_n}\right)^{-1/n} \times \left[\frac{96\pi^2 \left(-2^{(n+8)/n} (n-3)^2 \Phi_Q^2 \left(4^{1/n} \left(S/\omega_n\right)^{1/n}\right)^{-2n} \left(S/\omega_n\right)^{4/n} / (n-1) - n\Phi_c^2\right)}{n^2 \omega_n^2} \right. \\ \left. - 16^{1/n} \Lambda (n+1) \left(\frac{S}{\omega_n}\right)^{2/n} + 3(n-1) \right] \tag{35}$$

In our assumptions, where $n = 2$ and $\Lambda = -1$, (35) reduces to

$$T = \frac{S - \pi\left(\Phi_c^2 + \Phi_Q^2 - 1\right)}{4\pi^{3/2}\sqrt{S}} \tag{36}$$

which is in agreement with the result of [51, 52] if we set $\Phi_Q = 0$. Now we are able to write easily

$$\left(\frac{\partial T}{\partial S}\right)_{\Phi_Q, \Phi_c} = \frac{-S - 3\pi\left(\Phi_c^2 + \Phi_Q^2 - 1\right)}{16\pi^{3/2} S^{5/2}} \tag{37}$$

$$\left(\frac{\partial^2 T}{\partial S^2}\right)_{\Phi_Q, \Phi_c} = \frac{S + \pi\left(\Phi_c^2 + \Phi_Q^2 - 1\right)}{8\pi^{3/2} S^{3/2}} \tag{38}$$

The solution of $(\partial T/\partial S)_{\Phi_Q, \Phi_c} = 0$ can be derived as

$$S_1 = -\pi\left(\Phi_c^2 + \Phi_Q^2 - 1\right) \tag{39}$$

where the condition $\Phi_c^2 + \Phi_Q^2 < 1$ should be verified to ensure that the entropy in (39) is positive. In the other case $\Phi_c^2 + \Phi_Q^2 > 1$, one cannot find meaningful root of the equation $(\partial T/\partial S)_{\Phi_Q, \Phi_c} = 0$. Substituting (39) into (38) we obtain the following constraint

$$\left(\frac{\partial^2 T}{\partial S^2}\right)_{\Phi_Q, \Phi_c}\Bigg|_{S=S_1} = \frac{1}{8\pi^3\left(-\Phi_c^2 - \Phi_Q^2 + 1\right)^{3/2}} > 0 \tag{40}$$

implying that no critical point is observed in the $T - S$ diagram. This observation differs from the result in the previous section where the charges are kept fixed, consolidating the assertion that the thermodynamics in the grand canonical ensemble is quite different from that in the canonical one. In Figure 3, we depict the Hawking temperature for both the cases $\Phi_c^2 + \Phi_Q^2 < 1$ and $\Phi_c^2 + \Phi_Q^2 > 1$ and one can see that there exists minimum temperature for the left panel. Substituting (39) into (36), the minimum temperature can be obtained as

$$T_{min} = \frac{\sqrt{-\Phi_c^2 - \Phi_Q^2 + 1}}{2\pi}. \tag{41}$$

However, the Hawking temperature increases monotonically in the right panel.

Having obtained the phase picture of the thermal entropy of the AdS-Maxwell-Yang-Mills black hole, the canonical/grand canonical ensemble, we will now revisit the phase structure of the entanglement entropy and two-point correlation function to see whether they have similar phase structure in each thermodynamical ensemble.

3. Phase Transitions of Einstein-Maxwell-Yang-Mills-AdS Black Holes in Holographic Picture

3.1. Holographic Entanglement Entropy. First, let us provide a concise review of some generalities about the holographic entanglement entropy. For a given quantum field theory described by a density matrix ρ, with A being some region of a Cauchy surface of spacetime and A^c standing for its complement, the von Neumann entropy traduces the entanglement between these two regions

$$S_A = -\mathrm{Tr}_A\left(\rho_A \log \rho_A\right), \tag{42}$$

with ρ_A being the reduced density matrix of given by A $\rho_A = \mathrm{Tr}_{A^c}(\rho)$. Ryu and Takayanagi propose a simple geometric way to evaluate the entanglement entropy as [53, 54]

$$S_A = \frac{\mathrm{Area}\left(\Gamma_A\right)}{4G_N}, \tag{43}$$

in which Γ_A denotes a codimension-2 minimal surface with boundary condition $\partial\Gamma_A = \partial A$ and G_N stands for the gravitational Newton's constant. In our black hole model we choose the region A to be a spherical cap on the boundary delimited by $\theta \leq \theta_0$, and the minimal surface can be parametrized by the function $r(\theta)$. According to definition of the area and (9) and (43), one can show that the holographic entanglement entropy is governed by

$$S_A = \frac{\omega_{n-2}}{4} \int_0^{\theta_0} r^{n-2} \sin^{n-2}\theta \sqrt{\frac{\left(r'\right)^2}{f(r)} + r^2}\, d\theta, \tag{44}$$

where the notation prime denotes the derivative with respect to θ; e.g., $r' \equiv dr/d\theta$. Treat (44) as a Lagrangian and solve the equation of motion given by

$$r'(\theta)^2 \left[\sin\theta r(\theta)^2 f'(r) - 2\cos\theta r'(\theta)\right] - 2r(\theta) f(r) \\ \cdot \left[r(\theta)\left(\sin\theta r''(\theta) + \cos\theta r'(\theta)\right) - 3\sin\theta r'(\theta)^2\right] \\ + 4\sin(\theta) r(\theta)^3 f(r)^2 = 0. \tag{45}$$

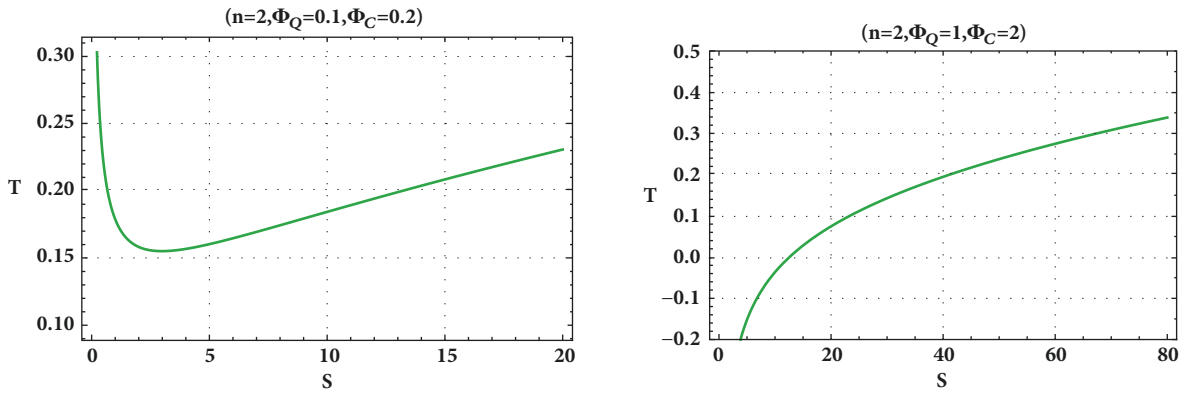

FIGURE 3: The temperature as a function of the entropy for different potentials. **(Left)** $\Phi_c^2 + \Phi_Q^2 < 1$. **(Right)** $\Phi_c^2 + \Phi_Q^2 > 1$.

Due to the difficulty to find an analytical form of the solution $r(\theta)$, we will perform a numerical calculation with adopting the following boundary conditions

$$r'(\theta) = 0, \quad r(0) = r_0. \tag{46}$$

Knowing that the entanglement entropy is divergent at the boundary, we regularized it by subtracting the area of the minimal surface in pure AdS whose boundary is also $\theta = \theta_0$ with

$$r_{AdS}(\theta) = L\left(\left(\frac{\cos\theta}{\cos\theta_0}\right)^2 - 1\right)^{-1/2}. \tag{47}$$

We label the regularized entanglement entropy by ΔS_A and for our numerical calculation we choose $\theta_0 = 0.2$ and 0.3 while Ultra Violet cutoff is chosen to be $\theta_c = 0.199$ and 0.299, respectively. To compare with the phase structure in the thermal picture, we will study the relation between the entanglement entropy and the Hawking temperature representing the temperature of the dual field theory; this relation is depicted in Figure 4 for different values of Maxwell's charge with a fixed Yang-Mills one near the critical point and the chosen θ_0.

For each panel, the red lines are associated with a charge less than the critical one while the ones equal to the critical charge are depicted in black dashed lines and green lines correspond to a charge upper than the critical one. Particularly, the first-order phase transition temperature $T_\star$ and second-order phase transition temperature T_c are plotted by magenta and orange dashed line, respectively. As can be seen in all these plots, the Van der Waals-like phase structure can also be observed in the $T - \Delta S_A$ diagram. Particularly, the coexistence temperature $T_\star$ and second-order phase transition temperature T_c are exactly the same as those in the thermal entropy structure.

Adopting the same steps as in the thermal picture, we will also check numerically whether Maxwell's equal area law holds

$$A_1 = \int_{\Delta S_A^{(1)}}^{\Delta S_A^{(2)}} T(\Delta S_A, Q)\, d\Delta S_A - T_*\left(\Delta S_A^{(2)} - \Delta S_A^{(1)}\right) \tag{48}$$

$$A_2 = T_*\left(\Delta S_A^{(3)} - \Delta S_A^{(2)}\right) - \int_{\Delta S_A^{(2)}}^{\Delta S_A^{(3)}} T(\Delta S_A, Q)\, d\Delta S_A \tag{49}$$

with the quantities $\Delta S_A^{(1)}$, $\Delta S_A^{(2)}$, and $\Delta S_A^{(3)}$ being roots of the equation $T_* = T(\Delta S_A, Q)$ in ascending order. The Maxwell's equal area law stipulates that

$$A_1 = A_2. \tag{50}$$

We tabulate in Table 3 the values of the both areas A_1 and A_2 for the chosen θ_0 and the charge C as well as the relative error between A_1 and A_2 taken to be the difference between A_1 and A_2 divided by their average.

Based on Table 3, we can see that, as the pressure approaches the critical one, the relative error which translates the disagreement between Maxwell's areas decreases. We can claim that the first-order phase transition of the holographic entanglement entropy obeys Maxwell's equal area law just near the critical point and within our numerical accuracy.

The next obvious step in our investigation is the check of the critical exponent of the second-order phase transition by analyzing the slope of the relation between $\log|T - T_c|$ and $\log|\Delta S_A - \Delta S_{A_c}|$, where ΔS_{A_c} is the critical entanglement entropy found numerically by an equation $T(\Delta S_A) = T_c$. We also introduce the definition of an analog to heat capacity by writing

$$\mathscr{C}_Q = T\left.\frac{\partial(\Delta S_A)}{\partial T}\right|_Q. \tag{51}$$

Taking $\theta_0 = 0.2$ and for different charge C, we plot the relationship between $\log|T - T_c|$ and $\log|\Delta S_A - \Delta S_{A_c}|$ inFigure 5, and the analytical relation can be fitted as

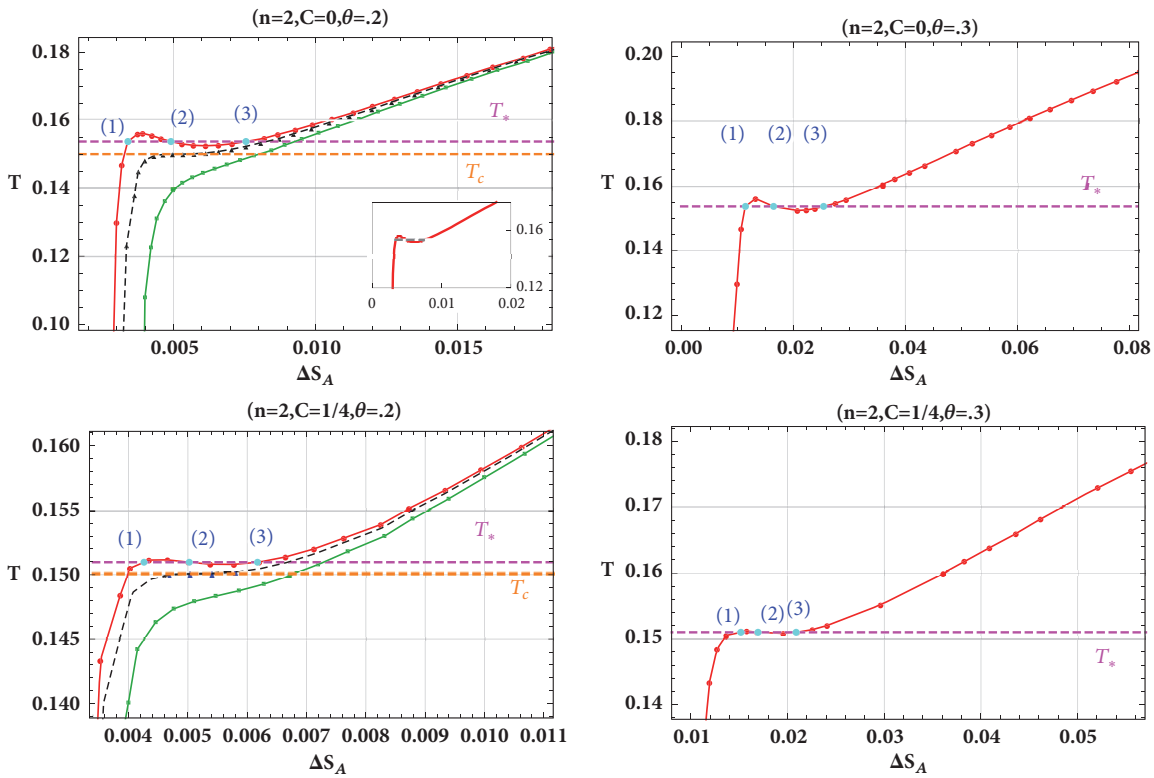

FIGURE 4: Plot of isocharges on the $(T, \Delta S_A)$-plan, for different values of θ_0, C. For all panels: the values of the charge are $Q = .9Q_c$ (red), $Q = Q_c$ (dashed black), and $Q = 2Q_c$ (green). The coexistence phase isotherm $T_\star$ (dashed magenta line) is obtained from the free energy (Figure 2) and the critical temperature (dashed orange line). For all curves, we also show the data points which are used to create the interpolation.

TABLE 3: Comparison of A_1 and A_2 for the EMPYM-AdS black hole using entanglement entropy.

C	$\frac{Q}{Q_c}$	θ_0	$\Delta S_A^{(1)}$	$\Delta S_A^{(2)}$	$\Delta S_A^{(3)}$	A_1	A_2	Relative error
0	**0.9**	0.2	0.00339417	0.00490769	0.00755095	2.271×10^{-6}	2.218×10^{-6}	2.36 %
		0.3	0.011477	0.0164978	0.0254236	6.563×10^{-6}	6.407×10^{-6}	2.4%
	0.5	0.2	0.00161291	0.0042458	0.0130777	0.00007432	0.00005560	28.81%
$\frac{1}{4}$	**0.9**	0.2	0.00425941	0.00502275	0.00617356	9.961×10^{-8}	1.023×10^{-7}	2.66%
		0.3	0.0151665	0.0169359	0.0208834	1.601×10^{-7}	1.631×10^{-7}	1.85%
	0.5	0.2	0.00339968	0.00496717	0.00743883	2.12718×10^{-6}	1.76781×10^{-6}	18.44%

$$\log|T - T_c| = \begin{cases} 14.2558 + \mathbf{3.09904} \log|\Delta S_A - \Delta S_{A_c}| & (C = 0) \\ 2.9293 + \mathbf{3.031061} \log|\Delta S_A - \Delta S_{A_c}| & \left(C = \frac{1}{4}\right) \end{cases} \quad (52)$$

The slope of (52) is around 3 indicating that the critical exponent is $-2/3$ in total concordance with that in (33); therefore the critical exponent for second-order phase transition of the holographic entanglement entropy agrees with that of the thermal entropy in the canonical ensemble [47, 50].

Now, we turn our attention to the grand canonical ensemble; we adopt the same analysis and the chosen values of the previous subsection, by writing (19) and (45) as a function of the potentials Φ_Q and Φ_c; taking the same boundary conditions (46), we perform the numerical calculations used in the plot of Hawking temperature as a function of the holographic entanglement entropy with fixed potentials in Figure 6.

Comparing Figure 3 with Figure 6, one may find that the thermal picture shares the same behavior of the holographic entanglement entropy; we can also observe the same minimum value of the temperature $T_{min} = 0.155125$. Then the holographic framework reproduces the same attitude of the $T - S$ diagram in the grand canonical ensemble.

Now, after showing that the holographic entanglement entropy shears the same phase picture as that of the thermal entropy for grand canonical and just near the critical point for the canonical ensemble since the relative disagreement between Maxwell's areas can become significantly large at low

Table 4: Comparison of A_1 and A_2 for the EMYM-AdS black hole using two-point correlation function.

C	$\frac{Q}{Q_c}$	θ_0	$\Delta L_A^{(1)}$	$\Delta L_A^{(2)}$	$\Delta L_A^{(3)}$	A_1	A_2	relative error
0	**0.9**	0.2	1.34978	1.34987	1.35003	0.000287	0.000300	4.42%
		0.3	0.881705	0.881911	0.882274	0.000197	0.000208	5.43%
	0.4	0.2	1.34967	1.34983	1.35043	0.001431	0.001812	23.49%
$\frac{1}{4}$	**0.9**	0.2	1.34983	1.34988	1.34995	0.000142	0.000138	2.85%
		0.3	0.881822	0.881926	0.882085	0.000209	0.000216	3.29%
	0.4	0.2	1.34978	1.34987	1.35003	0.0003907	0.0004653	17.42%

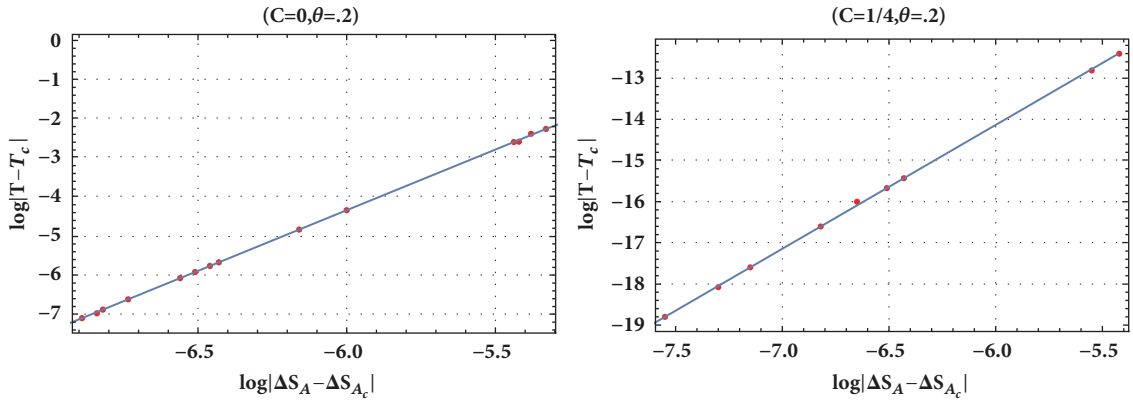

Figure 5: The relation between $\log|T - T_c|$ and $\log|\Delta S_A - \Delta S_{A_c}|$ for different C. **(Left)** $C = 0$. **(Right)** $C \neq 0$.

pressure, we attempt in the next section to explore whether the two-point correlation function has similar behavior to that of the entanglement entropy.

3.2. Two-Point Correlation Function. According to the Anti-de-Sitter/conformal fields theory correspondence, the time two-point correlation function can be written under the saddle-point assumption and in the large limit of Δ as [55]

$$\left\langle \mathcal{O}\left(t_0, x_i\right) \mathcal{O}\left(t_0, x_j\right)\right\rangle \approx e^{-\Delta L}, \tag{53}$$

where Δ is the conformal dimension of the scalar operator $\mathcal{O}$ in the dual field theory and the quantity L stands for the length of the bulk geodesic between the points (t_0, x_i) and (t_0, x_j) on the AdS boundary. Taking into account the symmetry of the considered black hole spacetime, we can simply use $x_i = \theta$ with the boundary θ_0 and employ it to parameterize the trajectory. In this case, the proper length can be expressed as

$$\begin{aligned} L &= \int_0^{\theta_0} \mathscr{L}\left(r\left(\theta\right), \theta\right) d\theta, \\ \mathscr{L} &= \sqrt{\frac{\left(r'\left(\theta\right)\right)^2}{f\left(r\left(\theta\right)\right)} + r\left(\theta\right)^2}, \quad \text{where } r' = \frac{dr}{d\theta} \end{aligned} \tag{54}$$

Treating $\mathscr{L}$ as Lagrangian and θ as time, one can write the equation of motion for $r(\theta)$ as

$$\begin{aligned} &r'\left(\theta\right)^2 f'\left(r\left(\theta\right)\right) - 2f\left(r\left(\theta\right)\right) r''\left(\theta\right) + 2r\left(\theta\right) f\left(r\left(\theta\right)\right)^2 \\ &\quad = 0. \end{aligned} \tag{55}$$

Recalling the boundary conditions of (46) we attempt to solve this equation by choosing the same background of the previous section, in other words the same values of the parameter θ_0 with the same UV cutoff values in the dual field theory. The regularized two-point correlation function is labeled as $\Delta L_A = L - L_0$, where L_0 denotes the geodesic length in pure AdS under the same boundary region. In Figure 7 we depict the behavior of the temperature T in function of ΔL_A; all plots show the Van der Waals-like phase transition as in the case of the thermal and the holographic entanglement entropy portrait.

As in the case of the holographic entanglement entropy, the relevant calculated results are listed in Table 4 which are the θ_0 values, the $\Delta\mathscr{L}_{A_{1,2,3}}$, and the areas A_1 and A_2.

The results of Table 4 tell us that under our numerical accuracy and just near the critical point Maxwell's equal area law still is verified implying that A_1 and A_2 are equal in the proximity to the critical pressure. These remarks consolidate the behavior of all panels of Figure 7. At this point, one can conclude that, like the entanglement entropy, the two-point correlation function also exhibits apparently a first-order phase transition as that of the thermal entropy. However, exploring broader ranges of the pressure has revealed the fact that the equal area law does not also hold.

For the second phase transition, we will be interested in the quantities $\log|T - T_c|$ and $\log|\Delta L_A - \Delta L_{A_c}|$ in which ΔL_{A_c} is obtained numerically by the equation $T(\Delta L_A) = T_c$. The

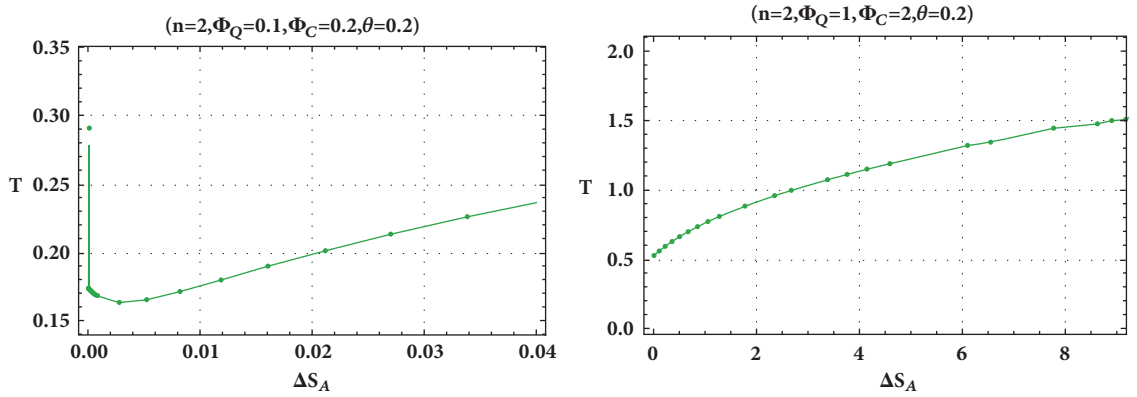

FIGURE 6: The relation between $\log|T - T_c|$ and $\log|\Delta S_A - \Delta S_{A_c}|$ for different C. **(Left)** ($\Phi_c = 0.1, \Phi_Q = 0.2$). **(Right)** ($\Phi_c = 1, \Phi_Q = 2$).

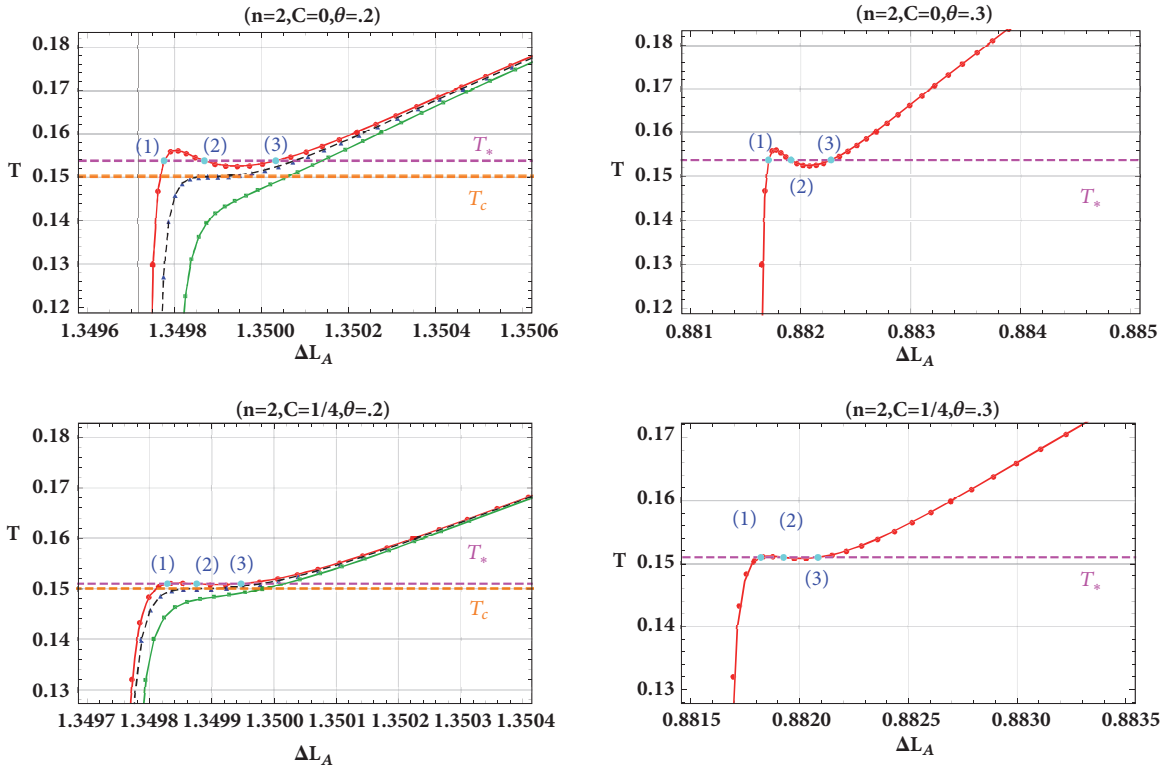

FIGURE 7: Plot of isocharges on the $(T, \Delta L_A)$-plan, for $C = 0$ (**left**) and $C \neq 0$ (**right**). For all panels: the values of the charge are $Q = 0.9Q_c$ (red), $Q = Q_c$ (dashed black), and $Q = 2Q_c$ (green).

relations between the logarithms of $|T - T_c|$ and $|\Delta L_A - \Delta L_{A_c}|$ are shown in Figure 8

The straight blue line in each panel of Figure 8 is fitted following the linear equations

$$\log|T - T_c| = \begin{cases} 19.056 + \mathbf{3.03594} \log\left|\Delta L_A - \Delta L_{A_c}\right| & (C = 0) \\ 14.25487 + \mathbf{3.04967} \log\left|\Delta L_A - \Delta L_{A_c}\right| & \left(C = \frac{1}{4}\right) \end{cases} \quad (56)$$

Again, we found a slope around 3; then the critical exponent of the specific heat capacity is consistent with that of the mean field theory of the Van der Waals as in the thermal and entanglement entropy portraits [47, 50]. Therefore, we conclude that the two-point correlation function of the Anti-de-Sitter-Maxwell-Yang-Mills black hole exists in a second-order phase transition at the critical temperature T_c.

For the grand canonical ensemble, we also plot the temperature T in function of ΔL_A in Figure 9, from which we can see that thermodynamical behavior is held as the thermal and the holographic entanglement entropy frameworks.

At this level we remark that radical rupture appears when we change the thermodynamical ensemble (canonical/grand canonical). The complete comprehension of such different

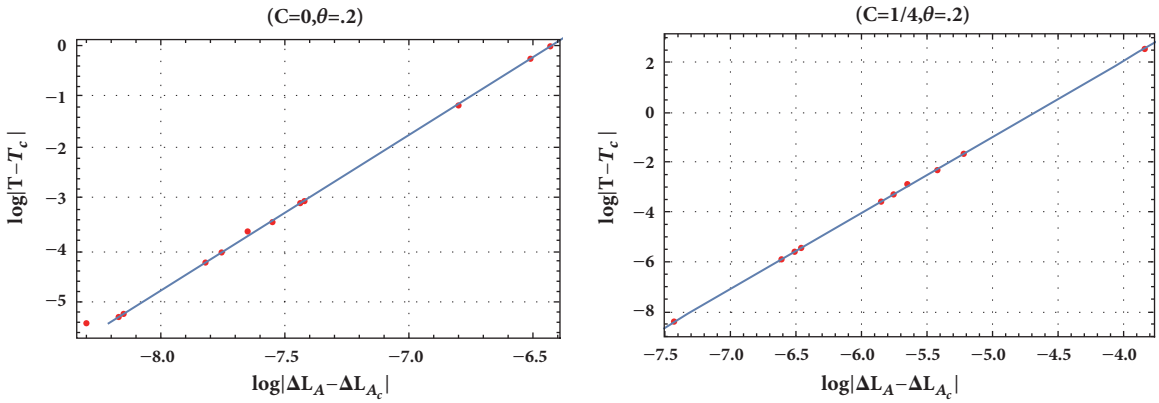

FIGURE 8: The relation between $\log|T - T_c|$ and $\log|\Delta L_A - \Delta L_{A_c}|$ for different charge C.

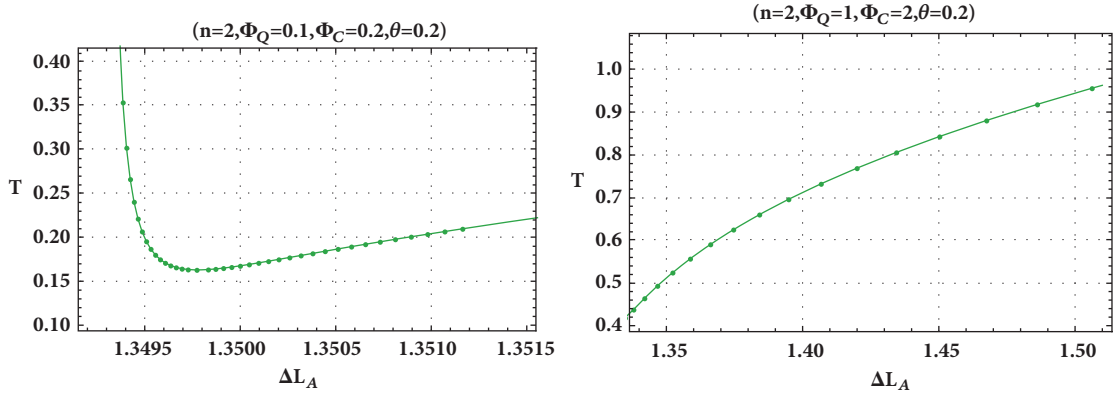

FIGURE 9: The relation between $\log|T - T_c|$ and $\log|\Delta S_A - \Delta S_{A_c}|$ for different C. **(Left)** ($\Phi_c = 0.1, \Phi_Q = 0.2$). **(Right)** ($\Phi_c = 1, \Phi_Q = 2$).

behaviors is not yet completely understood. We believe that it is typical of such system [41].

4. Conclusion

In this work We have investigated the phase transition of Anti-de-Sitter black hole in the Einstein-Maxwell-Yang-Mills gravity considering the canonical and the grand canonical ensemble. We first studied the phase structure of the thermal entropy in the (T, S)-plane for fixed charges and found that the phase structure agrees with the study made in [47] when the electrodynamics is linear. The authors consider the thermodynamics of such black hole in the (P, V)-plane, notably the critical behavior and the analogy with the Van der Waals gas. We also have shown that this behavior disappears in the grand canonical ensemble where the potentials Φ_Q and Φ_c are kept fixed.

Then, we found that this phase structure of the EMYM-AdS black hole can be probed by the two-point correlation function and holographic entanglement entropy in each thermodynamical ensemble, which reproduce the same thermodynamical behavior of the thermal portrait just for a range of the pressure near the critical one where the equal area law holds within our numerical accuracy; for broader ranges the disagreement between Maxwell's areas becomes significant. These remarks remain open questions while this approach provides a new step in our understanding of the black hole phase structure from the point of view of holography. Considering the high dimensional solutions or additional hairs by adding Yang-Mills fields and taking into account their confinement can be the object of a future publication.

Data Availability

The data used to support the findings of this study are available from the corresponding author upon request.

Conflicts of Interest

The author declares that they have no conflicts of interest.

References

[1] J. Maldacena, "The large N limit of superconformal field theories and supergravity," *International Journal of Theoretical Physics*, vol. 38, no. 2, Article ID 1113, 1999, [Advances in Theoretical and Mathematical Physics, vol. 2, p. 231, 1998].

[2] O. Aharony, S. S. Gubser, J. Maldacena, H. Ooguri, and Y. Oz, "Large N field theories, string theory and gravity," *Physics Reports*, vol. 323, no. 3-4, pp. 183–386, 2000.

[3] A. Hashimoto and N. Itzhaki, "Non-commutative Yang-Mills and the AdS/CFT correspondence," *Physics Letters. B. Particle Physics, Nuclear Physics and Cosmology*, vol. 465, no. 1-4, pp. 142–147, 1999.

[4] M. Faizal, A. F. Ali, and A. Nassar, "AdS/CFT correspondence beyond its supergravity approximation," *International Journal of Modern Physics A*, vol. 30, no. 30, p. 1550183, 2015.

[5] S. A. Hartnoll, "Lectures on holographic methods for condensed matter physics," *Classical and Quantum Gravity*, vol. 26, no. 22, 224002, 61 pages, 2009.

[6] A. Chamblin, R. Emparan, C. V. Johnson, and R. C. Myers, "Charged AdS black holes and catastrophic holography," *Physical Review D: Particles, Fields, Gravitation and Cosmology*, vol. 60, no. 6, Article ID 064018, 1999.

[7] S. W. Hawking and D. N. Page, "Thermodynamics of black holes in anti-de Sitter space," *Communications in Mathematical Physics*, vol. 87, no. 4, pp. 577–588, 1982/83.

[8] D. Kastor, S. Ray, and J. Traschen, "Enthalpy and the mechanics of AdS black holes," *Classical and Quantum Gravity*, vol. 26, no. 19, Article ID 195011, 16 pages, 2009.

[9] D. Kubiznak and R. B. Mann, "P-V criticality of charged AdS black holes," *Journal of High Energy Physics*, vol. 2012, no. 7, article 033, 2012.

[10] A. Belhaj, M. Chabab, H. E. Moumni, and M. B. Sedra, "On thermodynamics of AdS black holes in arbitrary dimensions," *Chinese Physics Letters*, vol. 29, no. 10, Article ID 100401, 2012.

[11] A. Belhaj, M. Chabab, H. El Moumni, K. Masmar, M. B. Sedra, and A. Segui, "On heat properties of AdS black holes in higher dimensions," *Journal of High Energy Physics*, vol. 2015, no. 5, Article ID 149, 2015.

[12] M. Chabab, H. El Moumni, and K. Masmar, "On thermodynamics of charged AdS black holes in extended phases space via M2-branes background," *The European Physical Journal C*, vol. 76, no. 6, Article ID 304, 2016.

[13] M. Chabab, H. El Moumni, S. Iraoui, K. Masmar, and S. Zhizeh, "Chaos in charged AdS black hole extended phase space," *Physics Letters B*, vol. 781, pp. 316–321, 2018.

[14] G.-M. Deng, J. Fan, X. Li, and Y.-C. Huang, "Thermodynamics and phase transition of charged AdS black holes with a global monopole," *International Journal of Modern Physics A*, vol. 33, no. 3, Article ID 1850022, 2018.

[15] S. H. Hendi, A. Sheykhi, and M. H. Dehghani, "Thermodynamics of higher dimensional topological charged AdS black branes in dilaton gravity," *The European Physical Journal C*, vol. 70, no. 3, pp. 703–712, 2010.

[16] Al Övgün I, "$P - v$ criticality of a specific black hole in *f(R)* gravity coupled with Yang-Mills field," *Advances in High Energy Physics*, vol. 2018, Article ID 8153721, 7 pages, 2018.

[17] J.-X. Mo, G.-Q. Li, and X.-B. Xu, "Combined effects of *f(R)* gravity and conformally invariant Maxwell field on the extended phase space thermodynamics of higher-dimensional black holes," *The European Physical Journal C*, vol. 76, no. 10, article no. 545, 2016.

[18] S. H. Hendi, S. Panahiyan, and B. Eslam Panah, "Extended phase space of black holes in Lovelock gravity with nonlinear electrodynamics," *PTEP. Progress of Theoretical and Experimental Physics*, no. 10, 103E01, 17 pages, 2015.

[19] M. H. Dehghani, S. H. Hendi, A. Sheykhi, and H. R. Sedehi, "Thermodynamics of rotating black branes in (n+1)-dimensional Einstein-Born-Infeld-dilaton gravity," *Journal of Cosmology and Astroparticle Physics*, vol. 2007, no. 2, article 020, 2007.

[20] H. E. Moumni, "Phase Transition of AdS Black Holes with Non Linear Source in the Holographic Framework," *International Journal of Theoretical Physics*, vol. 56, no. 2, pp. 554–565, 2017.

[21] H.-L. Li, S.-Z. Yang, and X.-T. Zu, "Holographic research on phase transitions for a five dimensional AdS black hole with conformally coupled scalar hair," *Physics Letters B*, vol. 764, pp. 310–317, 2017.

[22] Y. Sun, H. Xu, and L. Zhao, "Thermodynamics and holographic entanglement entropy for spherical black holes in 5D Gauss-Bonnet gravity," *Journal of High Energy Physics*, vol. 2016, no. 9, Article ID 060, 2016.

[23] S. He, L. F. Li, and X. X. Zeng, "Holographic van der waals-like phase transition in the Gauss–Bonnet gravity," *Nuclear Physics B*, vol. 915, pp. 243–261, 2017.

[24] J.-X. Mo, G.-Q. Li, Z.-T. Lin, and X.-X. Zeng, "Revisiting van der Waals like behavior of *f(R)* AdS black holes via the two point correlation function," *Nuclear Physics. B. Theoretical, Phenomenological, and Experimental High Energy Physics. Quantum Field Theory and Statistical Systems*, vol. 918, pp. 11–22, 2017.

[25] C. V. Johnson, "Large N phase transitions, finite volume, and entanglement entropy," *Journal of High Energy Physics*, vol. 2014, article 47, 2014.

[26] E. Caceres, P. H. Nguyen, and J. F. Pedraza, "Holographic entanglement entropy and the extended phase structure of STU black holes," *Journal of High Energy Physics*, vol. 2015, no. 9, article no. 184, 2015.

[27] P. H. Nguyen, "An equal area law for holographic entanglement entropy of the AdS-RN black hole," *Journal of High Energy Physics*, vol. 2015, article 139, 2015.

[28] X. X. Zeng and L. F. Li, "Van der waals phase transition in the framework of holography," *Physics Letters B*, vol. 764, pp. 100–108, 2017.

[29] J. X. Mo, G. Q. Li, Z. T. Lin, and X. X. Zeng, "Van der Waals like behavior and equal area law of two point correlation function of f(R) AdS black holes," *Nuclear Physics B*, vol. 918, pp. 11–22, 2017.

[30] S. Kundu and J. F. Pedraza, "Aspects of holographic entanglement at finite temperature and chemical potential," *Journal of High Energy Physics*, vol. 2008, no. 8, Article ID 177, 2016.

[31] H. El Moumni, "Revisiting the phase transition of AdS-Maxwellpower-YangMills black holes via AdS/CFT tools," *Physics Letters B*, vol. 776, p. 124, 2018.

[32] E. Yaraie, H. Ghaffarnejad, and M. Farsam, "Complexity growth and shock wave geometry in AdS-Maxwell-power-Yang–Mills theory," *The European Physical Journal C*, vol. 78, no. 11, 2018.

[33] X. X. Zeng, H. Zhang, and L. F. Li, "Phase transition of holographic entanglement entropy in massive gravity," *Physics Letters B*, vol. 756, p. 170, 2016.

[34] J. X. Mo, "An alternative perspective to observe the critical phenomena of dilaton AdS black holes," *The European Physical Journal C*, vol. 77, p. 529, 2017.

[35] D. Kubiznak, R. B. Mann, and M. Teo, "Black hole chemistry: thermodynamics with lambda," *Classical and Quantum Gravity*, vol. 34, no. 6, Article ID 063001, 2017.

[36] X.-X. Zeng and L.-F. Li, "Holographic Phase Transition Probed by Nonlocal Observables," *Advances in High Energy Physics*, vol. 2016, Article ID 6153435, 13 pages, 2016.

[37] J. Couch, W. Fischler, and P. H. Nguyen, "Noether charge, black hole volume, and complexity," *Journal of High Energy Physics*, vol. 2017, no. 3, Article ID 119, 2017.

[38] X.-X. Zeng and Y.-W. Han, "Holographic van der Waals Phase Transition for a Hairy Black Hole," *Advances in High Energy Physics*, vol. 2017, Article ID 2356174, 8 pages, 2017.

[39] A. Dey, S. Mahapatra, and T. Sarkar, "Thermodynamics and entanglement entropy with Weyl corrections," *Physical Review D: Particles, Fields, Gravitation and Cosmology*, vol. 94, no. 2, Article ID 026006, 2016.

[40] D. Dudal and S. Mahapatra, "Interplay between the holographic QCD phase diagram and entanglement entropy," *Journal of High Energy Physics*, vol. 2018, no. 7, Article ID 1807, 2018.

[41] A. Belhaj and H. El Moumni, "Entanglement entropy and phase portrait of f(R)-AdS black holes in the grand canonical ensemble," *Nuclear Physics. B. Theoretical, Phenomenological, and Experimental High Energy Physics. Quantum Field Theory and Statistical Systems*, vol. 938, pp. 200–211, 2019.

[42] G. L. Giordano and A. R. Lugo, "Holographic phase transitions from higgsed, non abelian charged black holes," *Journal of High Energy Physics*, vol. 2015, no. 7, Article ID 172, 172 pages, 2015.

[43] S. S. Gubser, "Breaking an Abelian gauge symmetry near a black hole horizon," *Physical Review D: Particles, Fields, Gravitation and Cosmology*, vol. 78, no. 6, Article ID 065034, 2008.

[44] S. S. Gubser, "Colorful horizons with charge in anti-de Sitter space," *Physical Review Letters*, vol. 101, no. 19, 191601, 4 pages, 2008.

[45] S. Gangopadhyay and D. Roychowdhury, "Analytic study of properties of holographic p-wave superconductors," *Journal of High Energy Physics*, vol. 2012, no. 8, Article ID 1208, 2012.

[46] S. Habib Mazharimousavi and M. Halilsoy, "Black Holes in Einstein-Maxwell-Yang-Mills Theory and their Gauss-Bonnet Extensions," *Journal of Cosmology and Astroparticle Physics*, vol. 2008, no. 12, Article ID 005, 2008.

[47] M. Zhang, Z.-Y. Yang, D.-C. Zou, W. Xu, and R.-H. Yue, "P-V criticality of AdS black hole in the Einstein-Maxwell-power-Yang-Mills gravity," *General Relativity and Gravitation*, vol. 47, no. 2, Article ID 14, 2015.

[48] A. B. Balakin, J. P. Lemos, and A. E. Zayats, "Regular nonminimal magnetic black holes in spacetimes with a cosmological constant," *Physical Review D: Particles, Fields, Gravitation and Cosmology*, vol. 93, no. 2, Article ID 024008, 2016.

[49] A. B. Balakin and A. E. Zayats, "Non-minimal Wu-Yang monopole," *Physics Letters. B. Particle Physics, Nuclear Physics and Cosmology*, vol. 644, no. 5-6, pp. 294–298, 2007.

[50] K. Bhattacharya, B. R. Majhi, and S. Samanta, "van der Waals criticality in AdS black holes: a phenomenological study," *Physical Review D: Particles, Fields, Gravitation and Cosmology*, vol. 96, no. 8, 084037, 8 pages, 2017.

[51] R. Banerjee, S. K. Modak, and D. Roychowdhury, "A unified picture of phase transition: from liquid-vapour systems to AdS black holes," *Journal of High Energy Physics (JHEP)*, vol. 1210, p. 125, 2012.

[52] R. Banerjee, S. Ghosh, and D. Roychowdhury, "New type of phase transition in Reissner Nordström-AdS black hole and its thermodynamic geometry," *Physics Letters B*, vol. 696, no. 1-2, pp. 156–162, 2011.

[53] S. Ryu and T. Takayanagi, "Holographic derivation of entanglement entropy from AdS/CFT," *Physical Review Letters*, vol. 96, Article ID 181602, 2006.

[54] S. Ryu and T. Takayanagi, "Aspects of holographic entanglement entropy," *Journal of High Energy Physics*, vol. 2006, no. 8, artcile 045, 2006.

[55] V. Balasubramanian and S. F. Ross, "Holographic particle detection," *Physical Review D: Particles, Fields, Gravitation and Cosmology*, vol. 61, no. 4, Article ID 044007, 2000.